CORE
Metadata, citation and similar papers at core.ac.uk
Provided by Elsevier - Publisher Connector

Available online at www.sciencedirect.com
ScienceDirect
Chinese Journal of Aeronautics 23(2010) 549-555

Chinese Journal of Aeronautics
www.elsevier.com/locate/cja

Sensitivity of MIMO STAP Radar with Waveform Diversity

Sun Jinping[a,*], Wang Guohua[b], Liu Desheng[c]

[a]*School of Electronics and Information Engineering, Beijing University of Aeronautics and Astronautics, Beijing 100191, China*

[b]*School of Electrical and Electronic Engineering, Nanyang Technological University, Singapore 639798, Singapore*

[c]*School of Automation Science and Electrical Engineering, Beijing University of Aeronautics and Astronautics, Beijing 100191, China*

Received 26 October 2009; accepted 12 January 2010

Abstract

Space-time adaptive processing (STAP) is an effective method adopted in airborne radar to suppress ground clutter. Multiple-input multiple-output (MIMO) radar is a new radar concept and has superiority over conventional radars. Recent proposals have been applying STAP in MIMO configuration to the improvement of the performance of conventional radars. As waveforms transmitted by MIMO radar can be correlated or uncorrelated with each other, this article develops a unified signal model incorporating waveforms for STAP in MIMO radar with waveform diversity. Through this framework, STAP performances are expressed as functions of the waveform covariance matrix (WCM). Then, effects of waveforms can be investigated. The sensitivity, i.e., the maximum range detectable, is shown to be proportional to the maximum eigenvalue of WCM. Both theoretical studies and numerical simulation examples illustrate the waveform effects on the sensitivity of MIMO STAP radar, based on which we can make better trade-off between waveforms to achieve optimal system performance.

Keywords: radar; MIMO; space-time adaptive processing; waveform diversity; sensitivity; waveform covariance matrix

1. Introduction

In recent years multiple-input multiple-output (MIMO) radar has shown superiority over conventional radar due to its ability of transmitting multiple correlated or uncorrelated waveforms via its antennas. More recently, the study of MIMO radar has been extended to space-time adaptive processing (STAP) for moving target indication (MTI)[1-6]. Conventional STAP systems can effectively suppress the ground clutter of inherent two-dimensional nature[7-8]. By applying STAP to a MIMO radar configuration, we can potentially increase the STAP ability to discriminate clutter as well as improve the target detection and estimation performances. In Refs.[1]-[6], the waveforms transmitted by separate transmitters are assumed to be orthogonal with each other. Thus it is possible for receiver to separate the signals from different transmitting antennas and utilize all degrees of freedom.

From a general point of view, one distinct property of MIMO radar is waveform diversity. In many applications, more general waveforms, i.e., correlated waveforms may be occupied by MIMO radar other than orthogonal waveforms. For example, by using partially correlated waveforms, the beam-shape of transmitting waveform can be optimized according to different purposes of application. Many articles are related to the design of these kinds of waveforms for MIMO radar based on different criteria[9-15]. To the best of our knowledge, when it comes to the partially correlated waveforms, the performance of MIMO STAP radar is not analyzed yet. Furthermore, to analyze the performance of MIMO STAP with waveform diversity can provide us more insight into MIMO radar and show both the advantages and disadvantages of certain waveforms. It can then guide us to select proper waveforms for the application of MIMO radar in certain practical operation, and show us how the radar performance is growing from the conventional coherent waveforms to orthogonal waveforms.

In this article, we start by constructing a signal model based on waveform diversity, i.e., transmitted waveforms are not constrained to be orthogonal. Performance metrics are then formulated and expressed as functions of the waveforms. With that, waveform effects on STAP performance can be studied from several perspectives. Then, the sensitivity, i.e., the maxi-

*Corresponding author. Tel.: +86-10-82317240.
E-mail address: sunjinping@buaa.edu.cn
Foundation items: National Natural Science Foundation of China (60901056); National Basic Research Program of China (6139303)

1000-9361 © 2010 Elsevier Ltd. Open access under CC BY-NC-ND license.
doi: 10.1016/S1000-9361(09)60253-3

mum range detectable, which is a metric of great importance for radar application, is analyzed. Though some articles pointed out that the MIMO radar will suffer from loss of transmitting power compared with single-input multiple-output (SIMO) radar[4], this article provides a general approach to evaluate the sensitivity of MIMO STAP radar with waveform diversity. It is achieved by investigating the effective transmitting-receiving (TR) gain and processing gain according to different waveforms. The sensitivity of MIMO STAP radar with waveform diversity is shown to be determined by eigenvalue distribution of the waveform covariance matrix (WCM) or waveform correlation matrix called in Ref.[15]. Along with it, we also compare the sensitivity of MIMO STAP applying orthogonal waveforms with conventional SIMO STAP.

2. Configurations and Signal Model

The MIMO radar system geometry is shown in Fig.1. In this article we use the same conventions as in Ref.[7]. The radar platform travels at velocity v_p in the positive direction of the x axis. The altitude of the array phase center is h over the Oxy plane. The surface of the earth is assumed to be flat for the interested area of observation. There are N omnidirectional transmitting elements uniformly spaced at distance d_{Tx}, and M receiving elements at distance d_{Rx}. As illustrated in Fig.1, the transmitting antennas are collocated with the receiving antennas, meaning that this system has a monostatic MIMO radar configuration. Thus, all the elements in the transmitting-receiving arrays view the target with the same azimuth and elevation angles. The elevation angle φ and azimuth angle θ are illustrated in Fig.1. At each transmitter, a coherent processing interval (CPI) consists of a sequence of L waveforms. Let $\boldsymbol{s}_n \in \mathbf{C}^{N_S \times 1}$ be the discrete baseband waveform transmitted at the nth transmitting element in each pulse repetition interval (PRI). Then, in each PRI, the transmitting waveform set is denoted by $\boldsymbol{S}=[\boldsymbol{s}_1 \ \boldsymbol{s}_2 \ \cdots \ \boldsymbol{s}_N]^{\mathrm{T}} \in \mathbf{C}^{N \times N_S}$. We also define the covariance matrix of transmitting waveforms as $\boldsymbol{R}_S=\boldsymbol{S}\boldsymbol{S}^{\mathrm{H}}/N_S \in \mathbf{C}^{N \times N}$. Orthogonal waveforms are defined as those satisfying $\boldsymbol{R}_S=\boldsymbol{I}_N$, where $\boldsymbol{I}_N$ is an identity matrix of size $N \times N$; coherent waveforms are defined as those satisfying $\boldsymbol{R}_S=\mathbf{1}_{N \times N}$, where $\mathbf{1}_{N \times N}$ is an N-dimension matrix with each element equal to one; waveforms other than orthogonal waveforms and coherent waveforms are defined as partially correlated waveforms. We assume that the transmitting waveforms meet the narrowband assumption. Thus the Doppler effect within the waveforms can be neglected. The pulse repetition interval is T_r and the waveform duration is T_p.

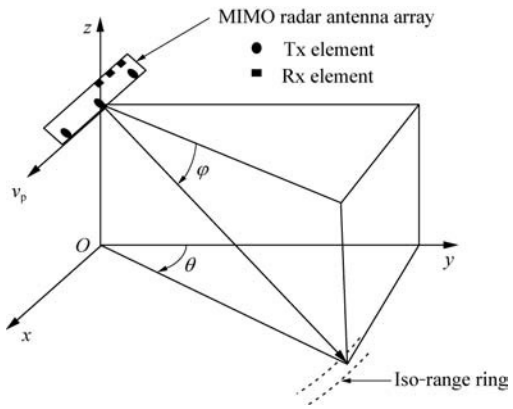

Fig.1 MIMO STAP system geometry.

After down-conversion, the echo for the lth PRI at the mth receiver from possible moving target and all clutter patches at the range ring of interest are

$$\boldsymbol{y}_m = \sum_{k=1}^{N} \gamma \boldsymbol{s}_k \mathrm{e}^{\mathrm{j}2\pi f_{s,t}[(k-1)\alpha+(m-1)]} \mathrm{e}^{\mathrm{j}2\pi f_{d,t}(l-1)} + \int_{\theta=0}^{2\pi} \sum_{k=1}^{N} \xi(\theta) \boldsymbol{s}_k \mathrm{e}^{\mathrm{j}2\pi f_{s,c}[(k-1)\alpha+(m-1)]} \mathrm{e}^{\mathrm{j}2\pi f_{d,c}(l-1)} \mathrm{d}\theta \quad (1)$$

where γ is the target reflection coefficient; $f_{s,t}=d_{Rx}\sin(\theta_t)\cos(\varphi_t)/\lambda$ and $f_{d,t}=2v_rT_r/\lambda$ are normalized target spatial and temporal frequencies, respectively, λ is the wavelength corresponding to the carrier frequency, θ_t the target azimuth angle, φ_t the target elevation angle, v_r the relative velocity between the target and platform; $f_{s,c}=d_{Rx}\sin(\theta)\cos(\varphi)/\lambda$ and $f_{d,c}=2\sin(\theta)\cos(\varphi)v_pT_r/\lambda$ are normalized spatial and temporal frequencies associated with the clutter of azimuth angle θ and elevation angle φ, respectively; $\alpha=d_{Tx}/d_{Rx}$; $\xi(\theta)$ is the signal amplitude from the clutter of angle θ. We also set $\beta=2v_pT_r/d_{Rx}$.

We can define a general transmitting steering vector and a receiving steering vector by

$$\boldsymbol{v}_{Tx}(\theta)=[1 \quad \mathrm{e}^{\mathrm{j}2\pi f_s\alpha} \quad \cdots \quad \mathrm{e}^{\mathrm{j}2\pi f_s\alpha(N-1)}]^{\mathrm{T}} \in \mathbf{C}^{N \times 1} \quad (2)$$

$$\boldsymbol{v}_{Rx}(\theta)=[1 \quad \mathrm{e}^{\mathrm{j}2\pi f_s} \quad \cdots \quad \mathrm{e}^{\mathrm{j}2\pi f_s(M-1)}]^{\mathrm{T}} \in \mathbf{C}^{M \times 1} \quad (3)$$

Define a Doppler vector as

$$\boldsymbol{u}(\theta)=[1 \quad \mathrm{e}^{\mathrm{j}2\pi f_d} \quad \cdots \quad \mathrm{e}^{\mathrm{j}2\pi(L-1)f_d}]^{\mathrm{T}} \in \mathbf{C}^{L \times 1} \quad (4)$$

To obtain the sufficient statistics for STAP signal processing, we can employ $\boldsymbol{\Phi}=\boldsymbol{S}^{\mathrm{H}}\boldsymbol{R}_S^{-1/2}$ as the filter bank in the receivers. It is common to diagonally load $\boldsymbol{R}_S$ before evaluating the inverse, in case $\boldsymbol{R}_S$ is singular in practical applications[11]. Thus the target echoes, the jamming signals and the clutter echoes are compressed by $\boldsymbol{\Phi}$ after filtering. Then the stacked data of target from angle θ_t is

$$\boldsymbol{\chi}_t=\boldsymbol{u}(\theta_t) \otimes \mathrm{stack}\left(\gamma \boldsymbol{v}_{Rx}(\theta_t)\boldsymbol{v}_{Tx}^{\mathrm{T}}(\theta_t)\boldsymbol{R}_S^{1/2}\right)= \gamma \boldsymbol{v}_t \in \mathbf{C}^{NML \times 1} \quad (5)$$

where $\boldsymbol{x}=\mathrm{stack}(\boldsymbol{X})$ defines a vector $\boldsymbol{x}$ formed by stacking the columns of the matrix $\boldsymbol{X}$, $\boldsymbol{v}_t$ is the target space-time steering vector, and $\otimes$ stands for the Kronecker product.

If the iso-range ring is divided in the cross-range dimension into N_c ($N_c \gg NML$) clutter patches, then the discrete form of the clutter data for the lth PRI is

$$\boldsymbol{x}_l=\text{stack}\left(\sum_{i=1}^{N_\text{c}}\xi(\theta_{\text{c},i})\text{e}^{\text{j}2\pi(l-1)f_{\text{c},i}}\boldsymbol{v}_\text{Rx}(\theta_{\text{c},i})\cdot \boldsymbol{v}_\text{Tx}^\text{T}(\theta_{\text{c},i})\boldsymbol{R}_\text{S}\right)\in\mathbf{C}^{NM\times 1} \tag{6}$$

where $f_{\text{c},i}=2\sin(\theta_{\text{c},i})\cos(\varphi)v_\text{p}T_\text{r}/\lambda$, $\theta_{\text{c},i}$ is the azimuth of the ith clutter patch, $\boldsymbol{v}_\text{Rx}(\theta_{\text{c},i})$ and $\boldsymbol{v}_\text{Tx}(\theta_{\text{c},i})$ are obtained from Eqs.(2)-(3) by substituting f_s with $f_{\text{s,c}}$, respectively, $\xi(\theta_{\text{c},i})$ can be modeled as a zero-mean independent complex Gaussian random variable with the variance σ_i^2. The clutter component of the space-time snapshot is then given by

$$\boldsymbol{\chi}_\text{c}=[\boldsymbol{x}_0\quad \boldsymbol{x}_1\quad \cdots\quad \boldsymbol{x}_{L-1}]^\text{T} \tag{7}$$

The ith clutter echoes from $\theta_{\text{c},i}$ can be stacked in the following form

$$\begin{aligned}\boldsymbol{\chi}_{\text{c},i}&=[\boldsymbol{x}_{0,i}\quad \boldsymbol{x}_{1,i}\quad \cdots\quad \boldsymbol{x}_{L-1,i}]^\text{T}=\\ &\xi_i\boldsymbol{u}(\theta_{\text{c},i})\otimes\text{stack}\left(\boldsymbol{v}_\text{Rx}(\theta_{\text{c},i})\boldsymbol{v}_\text{Tx}^\text{T}(\theta_{\text{c},i})\boldsymbol{R}_\text{S}^{1/2}\right)=\\ &\xi_i\boldsymbol{u}(\theta_{\text{c},i})\otimes\{[(\boldsymbol{R}_\text{S}^{1/2})^\text{T}\otimes\boldsymbol{v}_\text{Rx}(\theta_{\text{c},i})]\boldsymbol{v}_\text{Tx}(\theta_{\text{c},i})\}\triangleq\\ &\xi_i\boldsymbol{v}_{\text{c},i}\in\mathbf{C}^{NML\times 1}\end{aligned} \tag{8}$$

where $\xi_i=\xi(\theta_{\text{c},i})$. Then we define

$$\left.\begin{aligned}&\boldsymbol{V}_\text{c}=[\boldsymbol{v}_{\text{c},1}\quad \boldsymbol{v}_{\text{c},2}\quad \cdots\quad \boldsymbol{v}_{\text{c},N_\text{c}}]\\ &\boldsymbol{\Xi}=\text{diag}(\xi_1^2,\xi_2^2,\cdots,\xi_{N_\text{c}}^2)\end{aligned}\right\} \tag{9}$$

The clutter covariance matrix (CCM) can be written as

$$\boldsymbol{R}_\text{c}=E(\boldsymbol{\chi}_\text{c}\boldsymbol{\chi}_\text{c}^\text{H})=\boldsymbol{V}_\text{c}\boldsymbol{\Xi}\boldsymbol{V}_\text{c}^\text{H} \tag{10}$$

For noise component, we assume the noise snapshot, $\boldsymbol{\chi}_\text{n}$, is temporally and spatially de-correlated after compression, then the noise covariance matrix is

$$\boldsymbol{R}_\text{n}=E(\boldsymbol{\chi}_\text{n}\boldsymbol{\chi}_\text{n}^\text{H})=\sigma^2\boldsymbol{I}_{NML} \tag{11}$$

where σ^2 is the noise power. For a jammer at θ_j and φ_j, we assume its temporal behavior as the thermal noise with the characteristics of a point target in the spatial domain. We define $f_{\text{s,j}}=d_\text{Rx}\sin(\theta_\text{j})\cos(\varphi_\text{j})/\lambda$ as the normalized spatial frequency. The spatial steering vector associated with the jammer is

$$\boldsymbol{v}_{\text{Rx,j}}=[1\quad \text{e}^{\text{j}2\pi f_{\text{s,j}}}\quad \cdots\quad \text{e}^{\text{j}2\pi f_{\text{s,j}}(M-1)}]^\text{T}\in\mathbf{C}^{M\times 1} \tag{12}$$

The jammer samples at the lth pulse interval have the form of $\boldsymbol{j}_l\in\mathbf{C}^{N_\text{S}\times 1}$. Based on the assumption that the jammer is uncorrelated temporally, we can obtain that $E(\boldsymbol{j}_l\boldsymbol{j}_{l+\Delta}^\text{H})=\varsigma\sigma^2\delta(\Delta)\boldsymbol{I}$, where ς is the jamming-to-noise ratio and $\delta(\Delta)$ means the value of Dirac delta function at Δ. Therefore, after filtering, there would be NM jamming outputs for PRI. The consequent jamming component of spatial snapshot is in the form of

$$\boldsymbol{x}_{\text{j},l}=\text{stack}\{\boldsymbol{v}_{\text{Rx,j}}(\theta_\text{j},\varphi_\text{j})[\boldsymbol{j}_l((l-1)T_\text{r}+\tau)]^\text{T}\boldsymbol{\Phi}\} \tag{13}$$

Then the jammer space-time snapshot is

$$\boldsymbol{\chi}_\text{j}=[\boldsymbol{x}_{\text{j},0}\quad \boldsymbol{x}_{\text{j},1}\quad \cdots\quad \boldsymbol{x}_{\text{j},L-1}]^\text{T} \tag{14}$$

For each pulse, the jamming output covariance matrix can be

$$\begin{aligned}&E(\boldsymbol{x}_{\text{j},l}\boldsymbol{x}_{\text{j},l'}^\text{H})=\\ &(\boldsymbol{\Phi}^\text{T}\otimes\boldsymbol{v}_{\text{Rx,j}}(\theta_\text{j},\varphi_\text{j}))\boldsymbol{I}\varsigma\sigma^2[\boldsymbol{\Phi}\otimes(\boldsymbol{v}_{\text{Rx,j}}(\theta_\text{j},\varphi_\text{j}))^\text{T}]=\\ &\varsigma\sigma^2[\boldsymbol{\Phi}^\text{T}\boldsymbol{\Phi}\otimes\boldsymbol{v}_{\text{Rx,j}}(\theta_\text{j},\varphi_\text{j})(\boldsymbol{v}_{\text{Rx,j}}(\theta_\text{j},\varphi_\text{j}))^\text{T}]=\\ &\varsigma\sigma^2\boldsymbol{R}_\text{j}\end{aligned} \tag{15}$$

Eq.(15) indicates that correlation property of jamming signal will not be affected by the waveform covariance matrix according to the filter bank definition. The jamming is temporally uncorrelated between pulses, thus

$$E(\boldsymbol{x}_{l_1}\boldsymbol{x}_{l_2}^\text{H})=\boldsymbol{0} \tag{16}$$

Thus, the covariance matrix of jamming is

$$\boldsymbol{R}_\text{j}=E(\boldsymbol{\chi}_\text{j}\boldsymbol{\chi}_\text{j}^\text{H})=\varsigma\sigma^2\boldsymbol{I}_L\otimes\boldsymbol{R}_\text{j} \tag{17}$$

The total space-time snapshot including target, clutter, jamming and noise can be

$$\boldsymbol{\chi}=\boldsymbol{\chi}_\text{t}+\boldsymbol{\chi}_\text{j}+\boldsymbol{\chi}_\text{c}+\boldsymbol{n}\triangleq\boldsymbol{\chi}_\text{t}+\boldsymbol{\chi}_\text{u} \tag{18}$$

where $\boldsymbol{\chi}_\text{u}$ is the undesired component, consists of clutter, jamming and noise. For the problem of detecting the target in a complex environment with clutter, jamming and noise, the optimum space-time filter under the maximum signal-to-interference-plus-noise ratio (SINR) criterion is found from Ref.[7]:

$$\left.\begin{aligned}&\max\frac{\left|\boldsymbol{W}^\text{H}\boldsymbol{v}_\text{t}\right|^2}{\boldsymbol{W}^\text{H}\boldsymbol{R}_\text{u}\boldsymbol{W}}\\ &\boldsymbol{W}^\text{H}\boldsymbol{W}=1\end{aligned}\right\} \tag{19}$$

Thus we can get

$$\left.\begin{aligned}&\boldsymbol{W}=\boldsymbol{R}_\text{u}^{-1}\boldsymbol{v}_\text{t}\\ &\boldsymbol{R}_\text{u}^{-1}=E(\boldsymbol{\chi}_\text{u}\boldsymbol{\chi}_\text{u}^\text{H})\end{aligned}\right\} \tag{20}$$

Based on the above signal model constructed, it can be seen that unlike conventional SIMO radar, the space-time snapshots of both target signal and clutter signal are affected not only by the array manifold, but also by the waveforms, i.e., covariance matrix of waveforms. MIMO radars with both orthogonal waveforms and coherent waveforms can be taken as a special form of the MIMO radar with waveform diversity. More importantly, many waveforms for orthogonal MIMO radar in practice are not ideally orthogonal at all. Through the formulas derived above, the effects of nonideal orthogonal waveforms can also be studied.

3. Sensitivity of MIMO STAP Radar

Sensitivity of radar is of great importance because it will determine the functional range of the radar. Radar sensitivity is conventionally evaluated by radar equa-

tion[16]. We here rewrite the radar equation as

$$R_{\max}^4 = \frac{E_t G_T G_R \sigma_t \lambda^2}{(4\pi)^3 k T_0 F (S/N)_1 L_s} = \frac{E_t G_{TR} \sigma_t \lambda^2}{(4\pi)^3 k T_0 F (S/N)_1 L_s} \quad (21)$$

where $R_{\max}$ is the maximum range detectable, G_{TR} the total transmitting-receiving gain, E_t the total energy contained in one waveform, σ_t the target cross-section, k Boltzmann's constant, T_0 a reference temperature, F the receiver noise figure, and L_s the system losses. For a received signal to be detectable, it has to be larger than the receiver noise by a factor denoted here as $(S/N)_1$. This value of signal-to-noise ratio $(S/N)_1$ is that required if only one pulse is present. From Eq.(21) we can see that the sensitivity of radar is proportional to the transmitting-receiving gain given other factors fixed. Meanwhile, in STAP radar, the maximum detection range is proportional to the gain of spatial and temporal coherent integration over all elements and pulses[7]. The gain of spatial coherent integration is just G_{TR} from the transmitting-receiving beamforming. The gain of temporal coherent integration over all pulses is determined by the number of pulses. Obviously, the temporal coherent integration gain would be the same for different kinds of waveforms. Thus, we will focus on the gain from spatial coherent integration.

Therefore, in this section we will study the sensitivity of MIMO STAP radar with diverse waveforms from the perspective of waveform effects on TR gain. We also compare the sensitivity of MIMO STAP to that of conventional SIMO STAP.

3.1. Waveform effect on TR gain

For a given system with waveform diversity, all parameters are fixed other than waveforms. Thus, G_{TR} varies according to different waveform sets. The following will show this consideration. For MIMO radar, the TR gain can be written as[17]

$$G_{TR}(\theta) = \frac{|\boldsymbol{v}_{Tx}^H(\theta)\boldsymbol{R}_S\boldsymbol{v}_{Tx}(\theta_t)|^2 |\boldsymbol{v}_{Rx}^H(\theta)\boldsymbol{v}_{Rx}(\theta_t)|^2}{\boldsymbol{v}_{Tx}^H(\theta)\boldsymbol{R}_S\boldsymbol{v}_{Tx}(\theta)} \quad (22)$$

where $|x|$ is the magnitude of scalar x. From Eq.(22) we can see that the transmitting-receiving gain of MIMO radar is the product of transmitting gain and the receiving gain. For STAP radar systems with given antenna configuration, G_{TR} can be optimized with respect to $\boldsymbol{R}_S$. Because $\boldsymbol{R}_S$ is positive semi-definite, it can be decomposed by singular value decomposition as $\boldsymbol{R}_S = \boldsymbol{U}^H\boldsymbol{\Lambda}^2\boldsymbol{U}$, where $\boldsymbol{\Lambda} = \mathrm{diag}(\lambda_1, \lambda_2, \cdots, \lambda_N)$ and $\lambda_1 \geq \lambda_2 \geq \cdots \geq \lambda_N$ are the singular values of $\boldsymbol{R}_S$. Then we have

$$G_{TR}(\theta) = \frac{|\boldsymbol{v}_{Tx}^H(\theta)\boldsymbol{R}_S\boldsymbol{v}_{Tx}(\theta_t)|^2 |\boldsymbol{v}_{Rx}^H(\theta)\boldsymbol{v}_{Rx}(\theta_t)|^2}{\boldsymbol{v}_{Tx}^H(\theta)\boldsymbol{R}_S\boldsymbol{v}_{Tx}(\theta)} = \frac{|\boldsymbol{v}_{Tx}^H(\theta)\boldsymbol{U}^H\boldsymbol{\Lambda}\boldsymbol{\Lambda}\boldsymbol{U}\boldsymbol{v}_{Tx}(\theta_t)|^2 |\boldsymbol{v}_{Rx}^H(\theta)\boldsymbol{v}_{Rx}(\theta_t)|^2}{\boldsymbol{v}_{Tx}^H(\theta)\boldsymbol{R}_S\boldsymbol{v}_{Tx}(\theta)} \leq$$

$$\frac{\|\boldsymbol{v}_{Tx}^H(\theta)\boldsymbol{U}^H\boldsymbol{\Lambda}\|^2 \|\boldsymbol{\Lambda}\boldsymbol{U}\boldsymbol{v}_{Tx}(\theta_t)\|^2 |\boldsymbol{v}_{Rx}^H(\theta)\boldsymbol{v}_{Rx}(\theta_t)|^2}{\boldsymbol{v}_{Tx}^H(\theta)\boldsymbol{R}_S\boldsymbol{v}_{Tx}(\theta)} =$$

$$\boldsymbol{v}_{Tx}^H(\theta_t)\boldsymbol{R}_S\boldsymbol{v}_{Tx}(\theta_t) |\boldsymbol{v}_{Rx}^H(\theta)\boldsymbol{v}_{Rx}(\theta_t)|^2 \quad (23)$$

where $\|\boldsymbol{x}\|$ is the 2-norm of vector $\boldsymbol{x}$ and inequality comes from the rule of Cauchy-Schwarz inequality. As the transmit steering vector has constant Euclidean norm, by applying property of Rayleigh quotient we can get

$$\boldsymbol{v}_{Tx}^H(\theta_t)\boldsymbol{R}_S\boldsymbol{v}_{Tx}(\theta_t) \leq \lambda_{\max}(\boldsymbol{R}_S) \quad (24)$$

From Eqs.(23)-(24), we can see that the maximum TR gain is proportional to the largest eigenvalue of WCM. Thus, waveforms that obtain the largest eigenvalue will have the maximum TR gain. The maximum value is obtained in the case of coherent waveforms, i.e., total energy of $\boldsymbol{R}_S$ is concentrated in one eigenvalue. While for orthogonal signals, G_{TR} will be decreased by a factor of 10lg N, because all eigenvalues are the same. Thus, TR gain of orthogonal waveform is only $1/N$ of coherent waveforms. Meanwhile, the TR gain of partially correlated waveforms may be better than that of orthogonal waveform but worse than that of coherent waveforms. Fig.2 illustrates the above analysis, where we have 10 antenna elements as both transmitters and receivers spaced by half wavelength. Target azimuth is 0°. Coherent waveforms, orthogonal waveforms and partially correlated waveforms are used in this example. The partially correlated waveforms are designed by the method of minimum sidelobe design described in Ref.[9]. The mainbeam is centered at 0°, and 3 dB mainbeam area is set to [−12°, 12°]. However, as the transmitting gain of the orthogonal waveform is uniform over all azimuth angles, the maximum TR gain of orthogonal waveforms will keep unchanged no matter what the target azimuth is (see Fig.3(a)). For coherent or partially correlated waveform, the maximum TR gain will be affected by the difference between the azimuths of transmitting beam and target (see Fig.3(b)). In this way, although orthogonal waveforms can provide much more degrees of freedom than correlated waveforms do, it will have

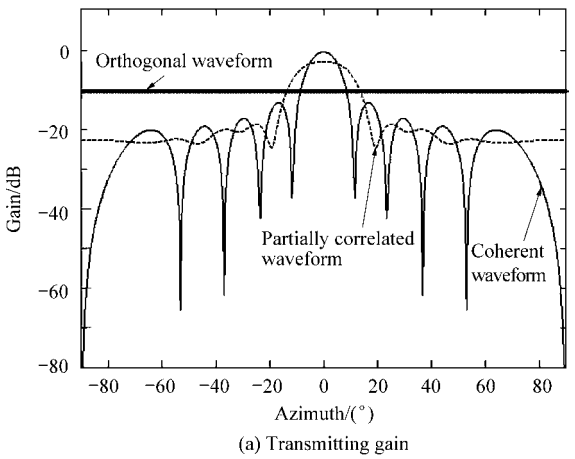

(a) Transmitting gain

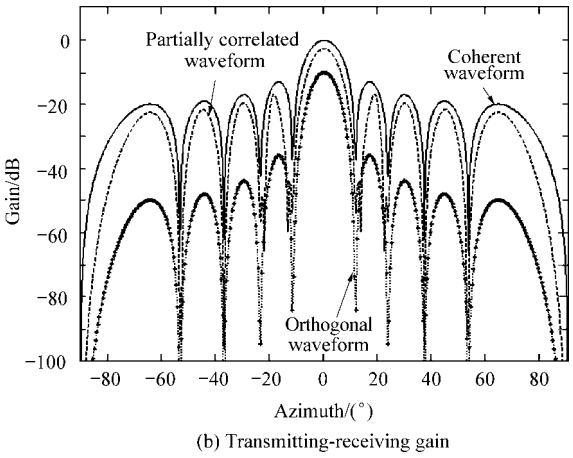

(b) Transmitting-receiving gain

Fig.2 Pattern for different waveforms.

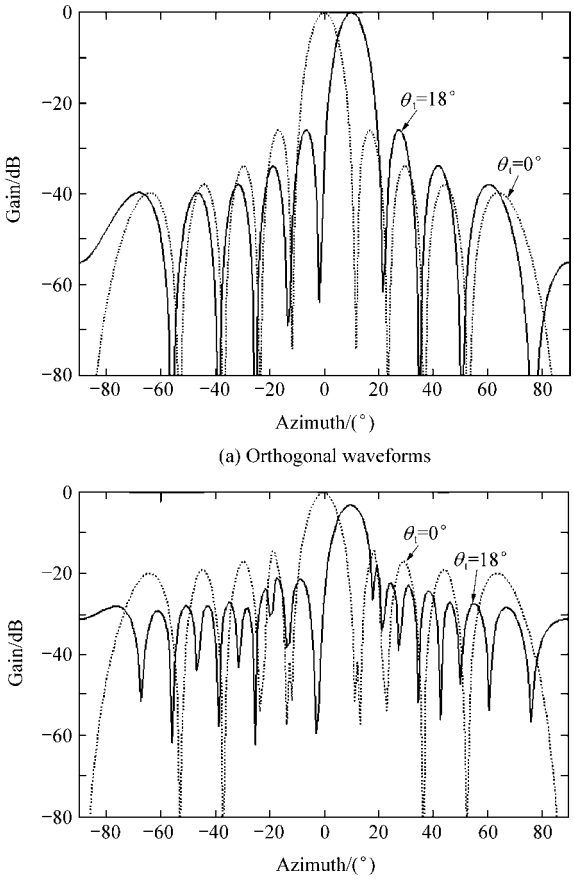

(a) Orthogonal waveforms

(b) Partially correlated waveforms

Fig.3 Pattern when target azimuth is different from that of transmitting and receiving.

lower TR gain. Meanwhile, although orthogonal waveform set has lower TR gain, it has better ubiquitous searching performance than other waveform sets because we only need to do the digital beamforming at the receiver end to cover all azimuth regions of interest in orthogonal waveform case.

The main reason for the appearance of asymmetric pattern in Fig.3(b) when the target is away from the boresight is that the partially correlated waveforms may lead to an asymmetric transmitting pattern for this target azimuth due to the un-uniform sampling property of the equivalent virtual array, which is determined by the eigenvalue (eigenvector) distribution of the waveform covariance matrix. Basically, for partially correlated waveform set, because its corresponding waveform covariance matrix has more complicated eigen-spectrum, discussion on the equivalent virtual array is not so clear and concise as that for the orthogonal waveforms. Therefore, the pattern should be better analyzed case-by-case to gain precise knowledge.

3.2. Waveform effect on processing gain and SINR

In this section, we will study the waveform effects on SINR metric and processing gain. Like the SINR loss defined and evaluated in Ref.[7], we here assess the processing gain by

$$\eta(f_{d,t}) = \frac{\mathrm{SINR}_{out}(f_{d,t})}{\mathrm{SNR}_{in}} \tag{25}$$

where SNR_{in} is the signal-to-noise ratio (SNR) that exists on each receiving element of the virtual array and is proportional to the TR gain, SINR_{out} $(f_{d,t})$ is the output SINR of STAP filter at normalized target temporal frequency $f_{d,t}$. We take the SNR_{in} of orthogonal waveform as 0 dB. From Eq.(25), the waveform effect can be investigated by holding the target angle fixed and varying the target Doppler frequency. Three kinds of waveforms are considered here, i.e., ideally orthogonal waveform, coherent waveform, and partially correlated waveform as previously mentioned. The system configuration is as follows: N=M=5, L=10, θ_t=0°, d_{Rx}=λ/2, α=5, v_p=100 m/s, v_t=70 m/s, β=1, λ=0.6 m, T_r=1.5 ms, B=10 MHz, the clutter-to-noise ratio is 30 dB and the jamming-to-noise ratio is 30 dB. Two jammer signals come from the directions of −40° and 30°, respectively. This configuration will be employed throughout the following content unless otherwise specified. The processing gain of MIMO radar has a maximum value of about 10lg(NML)=24.0 dB for all kinds of waveforms (see Fig.4). The gain of NML

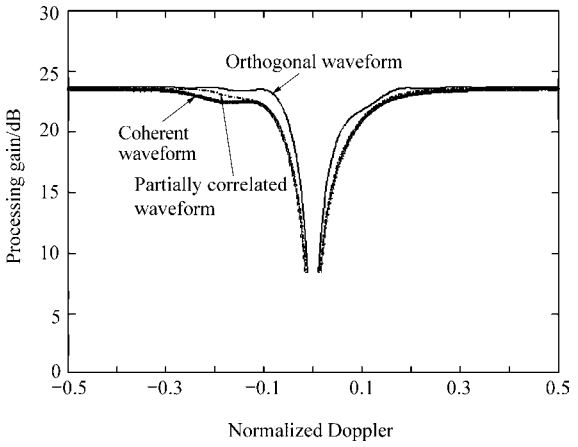

Fig.4 MIMO STAP processing gain of different waveforms (N=M=5, L=10).

represents coherent spatial and temporal integration over NM virtual elements and L pulses. This result can be explained and further generalized from a physical perspective that the processing gain for different waveforms would be the same because the total potential power for coherent spatial and temporal integration is the same for different waveforms. However, the orthogonal waveform set has the best velocity detectability as it has the narrowest clutter notch, while the coherent waveform set has the worst (see also Fig.4).

Based on both G_{TR} and processing gain, we can conclude that sensitivity of MIMO radar with waveform diversity is proportional to the maximum eigenvalue of the WCM. Specifically, the sensitivity of orthogonal waveform is only $1/N$ of the sensitivity of coherent waveform; the sensitivity of partially correlated waveforms may be better than that of orthogonal waveform but worse than that of coherent waveform. Thus MIMO radar may sacrifice the sensitivity for better velocity detectability and better spatial resolution capability owing to more degrees of freedom.

We can also compare the sensitivity of MIMO STAP between orthogonal waveform and conventional SIMO STAP. As for the conventional STAP, beamforming is conducted during transmitting. While for MIMO STAP with orthogonal waveform, beamforming will be performed after receiving. Thus, if SIMO STAP has the same number of transmitters as that of MIMO STAP, i.e., the same total transmit power, the $\mathrm{SNR}_{\mathrm{in}}$ of SIMO STAP ($\mathrm{SNR}_{\mathrm{in}}^{\mathrm{SIMO}}$) will be $N\times N$ times of the $\mathrm{SNR}_{\mathrm{in}}$ of MIMO radar $\mathrm{SNR}_{\mathrm{in}}^{\mathrm{MIMO}}$. We denote the $\mathrm{SINR}_{\mathrm{out}}$ of MIMO and SIMO as $\mathrm{SINR}_{\mathrm{out}}^{\mathrm{MIMO}}$ and $\mathrm{SINR}_{\mathrm{out}}^{\mathrm{SIMO}}$, the processing gain of MIMO and SIMO as η_{MIMO} and η_{SIMO}. If the pulse number is L for MIMO radar and SIMO radar, then the comparison of sensitivity can be illustrated by the ratio between the output SINRs of MIMO radar and SIMO radar as follows:

$$\frac{\mathrm{SINR}_{\mathrm{out}}^{\mathrm{MIMO}}}{\mathrm{SINR}_{\mathrm{out}}^{\mathrm{SIMO}}}=\frac{\mathrm{SNR}_{\mathrm{in}}^{\mathrm{MIMO}}}{\mathrm{SNR}_{\mathrm{in}}^{\mathrm{SIMO}}}\cdot\frac{\eta_{\mathrm{MIMO}}}{\eta_{\mathrm{SIMO}}}=\frac{1}{N^2}\cdot\frac{NML}{NL}=\frac{M}{N^2} \tag{26}$$

Compared with SIMO STAP, the total sensitivity of MIMO STAP with orthogonal waveform will decrease as long as $M<N^2$. Fig.5 shows the output SINRs of MIMO with $N=M=10$ and SIMO with $N=0$, $L=10$ for both. In this example, the output SINR of MIMO is approximately 10 dB less than the output SINR of SIMO.

Therefore, in practical operation, the sensitivity loss of MIMO radar with orthogonal waveforms must be compensated by improving the integration time for some applications in order to achieve equivalent performance as SIMO radar. The final sensitivity of MIMO radar after integrating can be calculated based on the available optimum integration time[18]. As described in Ref.[18], the optimum integrating time can be seriously limited by transmitter spurious-frequency spread and target modulation; the advantage of integration may not be fully realized. Thus, the sensitivity of MIMO radar should be carefully treated before practical application.

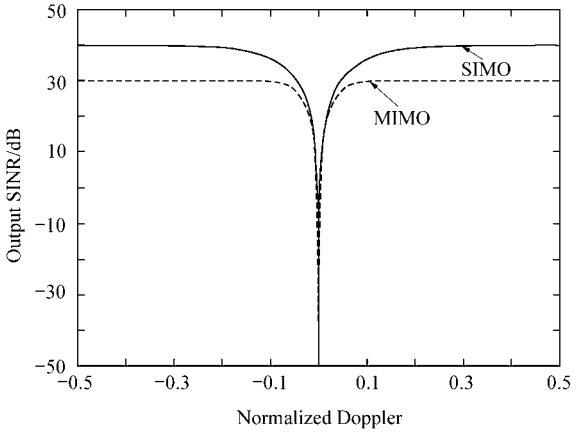

Fig.5 Output SINR comparison of MIMO and conventional SIMO STAP processor (N=M=10 for MIMO, N=10 for SIMO, L=10 for both).

4. Conclusions

In this article, we presented a general approach to evaluate the sensitivity of MIMO STAP radar with waveform diversity. The sensitivity of MIMO STAP radar with waveform diversity is found to be related to the eigenvalue distribution of the waveform covariance matrix. Simulation examples were provided to illustrate the analysis and conclusions. Based on the studies and conclusions we can balance different kinds of waveforms to achieve optimal system performance.

References

[1] Bliss D W, Forsythe K W. Multiple-input multiple-output (MIMO) radar and imaging: degrees of freedom and resolution. Conference Record of the Thirty-seventh Asilomar Conference on Signals, Systems and Computers. 2003; 54-59.

[2] Chen C Y, Vaidyanathan P P. A subspace method for MIMO radar space-time adaptive processing. Proceedings of ICASSP-2007. 2007; 925-928.

[3] Chen C Y, Vaidyanathan P P. Beamforming issues in modern MIMO radars with Doppler. Conference Record of the Fortieth Asilomar Conference on Signals, Systems and Computers. 2006; 41-45.

[4] Chen C Y, Vaidyanathan P P. MIMO radar space time adaptive processing using prolate spheroidal wavefunctions. IEEE Transactions on Signal Processing 2008; 56(2): 623-635.

[5] Mecca V, Ramakrishnan D, Krolik J. MIMO radar space-time adaptive processing for multipath clutter mitigation. Proceedings of Fourth IEEE Workshop on Sensor Array and Multichannel Processing. 2006; 249-253.

[6] Mecca V, Krolik J, Robey F. Beamspace slow-time

MIMO radar for multipath clutter mitigation. Proceedings of ICASSP-2008. 2008; 2313-2316.
[7] Ward J. Space-time adaptive processing for airborne radar. Technical Report ADA293032, 1994.
[8] Klemm R. Space-time adaptive processing: principles and applications. London: IEE Press, 1988.
[9] Stoica P, Li J, Xie Y. On probing signal design for MIMO radar. IEEE Transactions on Signal Processing 2007; 55(8): 4151-4161.
[10] Antonio G S, Fuhrmann D R, Robey F C. Transmit beamforming for MIMO radar systems using partial signal correlation. Conference Record of the Thirty-eighth Asilomar Conference on Signals, Systems and Computers. 2004; 295-299.
[11] Forsythe K W, Bliss D W. Waveform correlation and optimization issues for MIMO radar. Conference Record of the Thirty-ninth Asilomar Conference on Signals, Systems and Computers. 2005; 1306-1310.
[12] Friedlander B. Waveform design for MIMO radars. IEEE Transactions on Aerospace and Electronic Systems 2007; 43(3): 1227-1238.
[13] Li J, Xu L, Stoica P, et al. Range compression and waveform optimization for MIMO radar: a Cramer-Rao bound based study. IEEE Transactions on Signal Processing 2008; 56(1): 218-232.
[14] Li J, Stoica P, Zhu X. MIMO radar waveform synthesis. Proceedings of IEEE Radar Conference. 2008; 1-6.
[15] Fuhrmann D R, Antonio G S. Transmit beamforming for MIMO radar systems using signal cross-correlation. IEEE Transactions on Aerospace and Electronic Systems 2008; 44(1): 171-186.
[16] Skolnik M. Radar handbook. 2nd ed. New York: McGraw-Hill; 1990.
[17] Bekkerman I, Tabrikian J. Target detection and localization using MIMO radars and sonars. IEEE Transactions on Signal Processing 2006; 54(10): 3873-3883.
[18] Flaherty J M, Kadak E. Optimum radar integration time. IRE Transactions on Antenna and Propagation 1960; 8(2): 183-185.

Biographies:

Sun Jinping Born in 1975, an associate professor at School of Electronics and Information Engineering of Beijing University of Aeronautics and Astronautics. He is engaged in high resolution and advance mode radar signal processing, image understanding and pattern recognition.
E-mail: sunjinping@buaa.edu.cn

Wang Guohua Born in 1979. He is currently a Ph.D. candidate at School of Electrical and Electronic Engineering, Nanyang Technological University, Singapore. His current research interests are in the areas of waveform design and diversity and MIMO radar signal processing.

Liu Desheng Born in 1970. He is currently an associate professor and a Ph.D. candidate at School of Automation Science and Electrical Engineering, Beijing University of Aeronautics and Astronautics. His current research interests are in the areas of avionics and signal processing.